The Meteoritical Society

Meteoritics & Planetary Science 43, Nr 4, 685–699 (2008)
Abstract available online at http://meteoritics.org

Noble gases in Grant and Carbo and the influence of S- and P-rich mineral inclusions on the ^{41}K-^{40}K dating system

Katja AMMON[1*], Jozef MASARIK[2], and Ingo LEYA[1]

[1]Physikalisches Institut, University of Bern, Sidlerstrasse 5, CH-3012 Bern, Switzerland
[2]Komensky University, Bratislava, Slovakia
[*]Corresponding author. E-mail: kammon@staffmail.ed.ac.uk

(Received 14 August 2007; revision accepted 14 March 2007)

Abstract–Cosmogenic He, Ne, and Ar were measured in the iron meteorites Grant (IIIAB) and Carbo (IID) to re-determine their preatmospheric geometries and exposure histories. We also investigated the influence of sulphur- and/or phosphorus-rich inclusions on the production rates of cosmogenic Ne. Depth profiles measured in Grant indicate a preatmospheric center location 117 mm left from the reference line and 9 mm below bar B, which is clearly different (~10 cm) from earlier results (~165 mm left from the reference line on bar F). For Carbo the preatmospheric center location was found to be 120 mm right of the reference line and 15 mm above bar J, which is in agreement with literature data. The new measurements indicate a spherical preatmospheric shape for both meteorites and, based on literature ^{36}Cl data, the radii were estimated to be about 32 cm and 70 cm for Grant and Carbo, respectively. We demonstrate that minor elements like S and P have a significant influence on the production rates of cosmogenic Ne. In our samples, containing on average 0.5% S and/or P, about 20% of ^{21}Ne was produced from these minor elements. Using measured ^{21}Ne concentrations and endmember $^{22}Ne/^{21}Ne$ ratios for Fe + Ni and S + P, respectively, we show that it is possible to correct for ^{21}Ne produced from S and/or P. The thus corrected data are then used to calculate new ^{41}K-^{40}K exposure ages—using published K data—which results in 564 ± 78 Ma for Grant and 725 ± 100 Ma for Carbo. The correction always lowers the ^{21}Ne concentrations and consequently decreases the ^{41}K-^{40}K exposure ages. The discrepancies between ^{36}Cl-^{36}Ar and ^{41}K-^{40}K ages are accordingly reduced. The existence of a significant long-term variation of the GCR, which is based on a former 30–50% difference between ^{41}K-^{40}K and ^{36}Cl-^{36}Ar ages, may warrant re-investigation.

INTRODUCTION

Cosmogenic nuclides are produced by interactions of galactic and solar cosmic-ray particles with terrestrial and extraterrestrial matter. In contrast to solar cosmic-rays, which have penetration depths of a very few cm only (e.g., Wieler 2002), galactic cosmic-rays (GCR) can penetrate deep (several tens of cm up to m) (e.g., Eugster 2003) into meteoroids and planetary bodies and thereby produce, among others, cosmogenic radionuclides and stable noble-gas isotopes. The production rates of cosmogenic nuclides depend on the shape of the GCR particle spectra, the total GCR flux, the geometry and chemistry of the meteoroid, and the position of the sample within the body (shielding depth). While the production systematics for stony meteorites and lunar surface rocks can reliably be calculated (Leya et al. 2000, 2001) there are still unresolved issues involving cosmogenic nuclide production systematics for iron meteorites.

For iron meteorites with $r \geq 10$ cm the flux densities of primary and secondary particles decrease (Wieler 2002; Leya et al. 2004 and ref. therein) from the surface towards the center, leading to decreasing production rates with increasing depth. The production rates also decrease with increasing size of the meteoroid. The exception to this are those nuclides produced by thermal and epithermal neutrons, in which case the production rates peak somewhat below the surface. In addition, the production rates mostly increase with decreasing mass difference between target element and product nuclide. For example, the production rates for cosmogenic $^{20, 21, 22}Ne$ from ^{32}S and ^{31}P are much higher than the corresponding production rates from the major target isotopes ^{56}Fe and ^{58}Ni. This is important because troilite (FeS) and schreibersite ($(Fe,Ni)_3P$) are common minerals in iron meteorites. However, the contributions of Ne isotopes from S and P have not been considered for production rate systematics in the past (e.g., Martin 1953; Ebert and Wänke 1957; Signer and Nier

1960, 1962; Arnold et al. 1961; Voshage and Feldmann 1979). Michlovich et al. (1994) noted that S might be an important target element for the production of ^{26}Al in Canyon Diablo.

In the early 1960s Signer and Nier (1960, 1962) measured noble gases in samples of the IIIAB iron meteorite Grant and found rather simple depth dependencies for cosmogenic He, Ne, and Ar isotopes as well as for some elemental ratios. Based on these results, the authors hypothesized a model from which the radius of the meteoroid (R), the shielding depth of the sample (d), and the exposure age (T_{exp}) could be determined from a single sample. Later, Voshage and Feldmann (1978, 1979) recognized that the Signer-Nier model is based only on two independent experimental results, the ^{4}He and the ^{21}Ne concentrations, demonstrating that R, d, and T_{exp} could not be uniquely determined from only these measurements. Consequently, for a proper determination of the preatmospheric geometry and the exposure history of iron meteorites the dependence of the production rates and the cosmogenic nuclide ratios on the meteoroid size, on the shielding depth of the studied sample, and on the chemistry has to be known. In addition, the exposure age of the meteoroid has to be determined independently (Voshage and Feldmann 1978).

Various approaches exist to determine cosmic-ray exposure ages of iron meteorites. The most widely used are the ^{41}K-^{40}K and the ^{36}Cl-^{36}Ar methods. The ^{41}K-^{40}K dating system has been developed by Voshage and co-workers (e.g., Voshage and Hintenberger 1961; Voshage 1962, 1978) and is based on the production rate ratios of the stable isotopes ^{39}K and ^{41}K and the radioactive isotope ^{40}K. The ^{36}Cl-^{36}Ar system is based on the fact that ^{36}Ar is the radioactive daughter of ^{36}Cl ($^{36}\text{Cl} \rightarrow {}^{36}\text{Ar} + e^{-} + \bar{\nu}$). In iron meteorites, more than 80% (Lavielle et al. 1999) of the ^{36}Ar measured today was originally produced as ^{36}Cl. Since ^{36}Cl ($T_{1/2}$ = 0.3 Ma) is in saturation after a few million years, its measured concentration is a very good proxy for the ^{36}Ar production rate, which makes this system very reliable (e.g., Lavielle et al. 1999; Wieler 2002). The ^{36}Cl-^{36}Ar system reflects the radiation conditions over the last few million years only, whereas the ^{41}K-^{40}K system gives an average age over the lifetime of the meteoroid. Exposure ages determined via ^{41}K-^{40}K have been found to be higher by about 30%–50% than those determined via ^{36}Cl-^{36}Ar (Voshage 1978, 1984; Lavielle et al. 1999). This finding has usually been interpreted as indicating an increase in the GCR flux in the last few million years. However, the ^{41}K-^{40}K system is based on many assumptions, which are not well tested, or not tested at all (e.g., the production rates of K). Therefore, the observed discrepancies might also be artifacts, indicating our insufficient knowledge of cosmogenic production systematics, rather than a long-term GCR variation.

Here we present new results for cosmogenic He, Ne, and Ar in samples of the IIIAB iron meteorite Grant and the IID iron meteorite Carbo. Based on our new data we have re-determined the preatmospheric center locations and radii for both meteorites, which are (at least for Grant) significantly different from earlier estimates (Hoffman and Nier 1958; Signer and Nier 1960). By studying the reproducibility of our measurements we clearly demonstrate that troilite and schreibersite inclusions significantly influence the measured Ne concentration in a given sample. This has to be considered when Ne production rates are being deduced from such data. Using the cosmogenic ^{21}Ne concentrations and suitable ^{22}Ne/^{21}Ne endmember ratios for Fe + Ni and S + P, it is possible to correct for such contributions. The results are then applied to the ^{41}K-^{40}K system and new exposure ages are determined for Grant and Carbo.

EXPERIMENTAL

Samples

Grant is a medium octahedrite and belongs to the group of the IIIAB iron meteorites. Several pieces were found in the 1920s in New Mexico. In 1957 the main mass was cut in 2 halves, and 2 central slices of about 1 cm thickness were produced (Buchwald 1975). These slices almost touched the preatmospheric center of the meteoroid. Carbo is also a medium octahedrite and belongs to the group of IID iron meteorites. A mass of 450 kg was found in Mexico in 1923. Similar to Grant, a central slice was cut out of the main mass in 1957 (Buchwald 1975). Figures 1a and 1b show the central slices of Carbo and Grant, respectively, which were further cut into several bars. The locations of all samples analyzed in this work are plotted on these bars.

Sample Preparation and Noble Gas Extraction

The samples, weighing 50–100 mg each, were ultrasonically cleaned in acetone and wrapped in Ni foil. The samples were preheated in vacuum to about 80 °C for 2 days to release atmospheric surface contamination. We measured 30 aliquots of Grant and 31 of Carbo. Two different instruments were used for sample measurements. For some samples the noble gases were extracted in a conductively heated crucible. After purification the noble gases were measured on a MAP 215-50 sector field mass spectrometer (90°, 15 cm radius) equipped with a Nier type ion source and 2 detectors, a Faraday cup and an electron multiplier operating in counting mode. Most samples were analyzed on a system in which the noble gases were released in a crucible heated by an RF coil. After purification the gases were admitted into a sector field mass spectrometer able to measure He and Ne and a tandem spectrometer for Ar measurements. These 2 non-commercial spectrometers are called system B

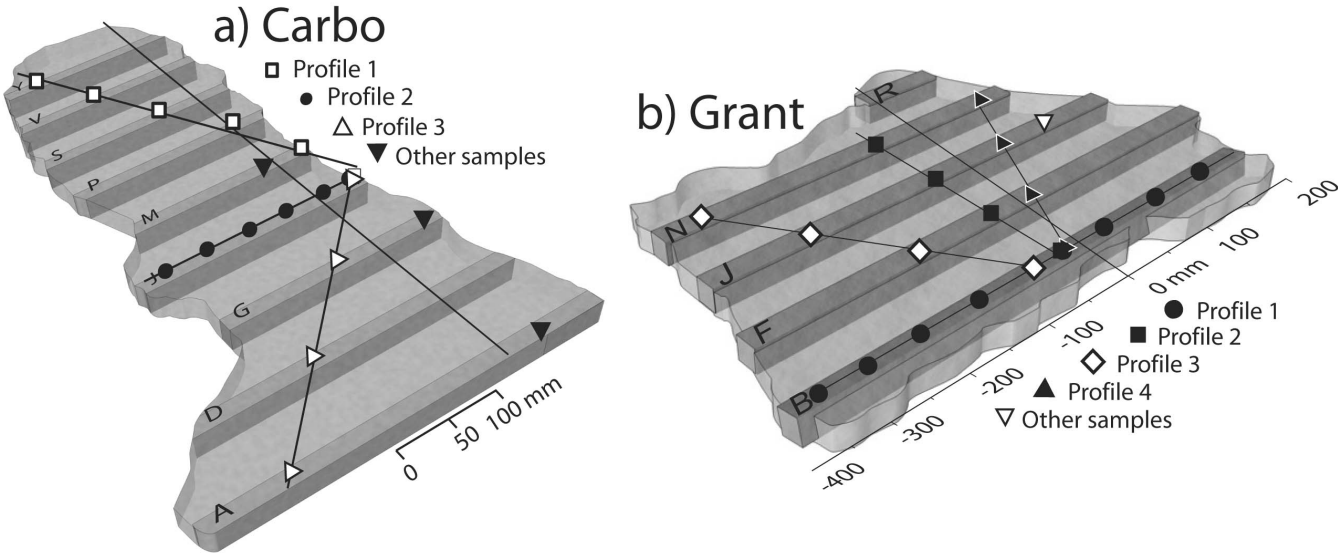

Fig. 1. The center slices of Carbo (a) and Grant (b) were cut into different bars labeled from A–Y and B–R, respectively. The measured depth profiles are distinguished using different symbols.

mass spectrometers (see e.g., Schwarzmüller 1970). They are equipped with a Nier type ion source, a Faraday cup, and an electron multiplier.

Since the results published here were mostly obtained on the second system (system B), this extraction line is described in some detail: samples are melted in a molybdenum crucible. To avoid corrosion, a boron-nitride liner (Maruoka and Matsuda 2001) is placed inside the Mo crucible. Noble gases are extracted by heating the samples slowly up to about 1670–1700 °C. This temperature, which is held for 20 min, is far above the melting point of Fe and Ni, but such a high temperature is needed to guarantee complete degassing, as we verified during various step-wise heating experiments. During melting, the gas is purified with 2 titanium (Ti) getters first held at about 700 °C and then cooling down to room temperature. Argon is separated from the He-Ne fraction using active charcoal held at the temperature of boiling nitrogen (LN_2). The He-Ne fraction is pumped towards the He-Ne spectrometer using a mercury (Hg) diffusion pump and is further purified using Ti-getters (400 °C—room temperature) and active charcoal (LN_2). During measurements an active charcoal (LN_2) and a Ti-getter (room temperature) in the spectrometer guarantee a low ^{40}Ar, CO_2, and HD background to minimize interferences on ^{20}Ne, ^{22}Ne, and ^{3}He, respectively. The Ar fraction is further purified using Ti-getters working in a temperature range between 700 °C and 200 °C. The gas is concentrated towards the Ar spectrometer using a further active charcoal (LN_2). During the release of Ar, the charcoal is cooled with CO_2 ice to retain contaminants like water and CO_2, which could compromise the Ar measurements.

Calibrations

The sensitivities and mass fractionations for all spectrometers used in this study were determined using calibrations composed of known amounts of He, Ne, and Ar isotopes. The data given in Tables 1 and 2 are all corrected for mass fractionation. On the MAP spectrometer we determined a mass discrimination on the counter of 2.3%/amu and 2.6%/amu for Ne and Ar respectively, favoring the light isotopes. The fractionation for the Ar measurements on the Faraday cup was negligible. For He the fractionation factor could not be determined directly because ^{3}He could not be measured in the calibration. The $^{3}He/^{4}He$ ratios of Grant samples were compared to the corrected replicates measured on the system B spectrometer and we observed a fractionation of about 10% favouring the heavy isotope.

The corrections for mass fractionation for the secondary electron multiplier (SEM) of the separate He-Ne and Ar spectrometers are 5%/amu, 3%/amu, and 2.3%/amu for He, Ne, and Ar, respectively, favoring the light isotope and it is 1% for Ar measured on the Faraday cup favoring the heavy isotope (He and Ne were measured only on the SEM). For He this factor is only valid for gas concentrations very close to the gas amount used for calibration. Extensive tests clearly demonstrated that the fractionation factor for He depends on the gas amount in the spectrometer. For example, some samples have up to 40 times more ^{4}He than a calibration, which lowers the fractionation from 5% to 1%. Also, the sensitivities for He, Ne, and Ar depend on the gas amount in the spectrometer. For He this can make up to 7% for typical samples. For Ne and Ar concentrations, the

Table 1. Helium, Ne, and Ar concentrations (in 10^{-8} cm^3 STP/g) for Grant. Neon-21 is not corrected for S + P contributions.

Bar	Distance from ref. line (mm)	Mass (mg)	Distance from center (mm)	$^4He \pm 2\sigma$	$^{21}Ne \pm 2\sigma$	$^{38}Ar \pm 2\sigma$	$^3He/^4He \pm 2\sigma$	$^{20}Ne/^{21}Ne \pm 2\sigma$	$^{22}Ne/^{21}Ne \pm 2\sigma$	$^{36}Ar/^{38}Ar \pm 2\sigma$
				(10^{-8} cm^3 STP/g)						
B[1]	–347	77.2	230	1820 ± 175	6.17 ± 0.44	31.64 ± 13	0.276 ± 0.001	0.898 ± 0.034	1.066 ± 0.010	0.629 ± 0.001
B[1]	–293	68.2	176	1761 ± 169	5.57 ± 0.36	30.31 ± 13	0.273 ± 0.001	0.933 ± 0.017	1.067 ± 0.009	0.626 ± 0.001
B[1]	–230	80.9	113	1692 ± 162	5.30 ± 0.34	28.66 ± 12	0.268 ± 0.002	0.922 ± 0.015	1.077 ± 0.020	0.624 ± 0.001
B[1]	–178	52.5	61	1625 ± 156	4.98 ± 0.45	27.36 ± 12	0.267 ± 0.001	0.910 ± 0.094	1.061 ± 0.012	0.625 ± 0.001
B[1]	–133	61.9	18	1673 ± 160	5.03 ± 0.34	28.02 ± 12	0.265 ± 0.003	0.915 ± 0.024	1.048 ± 0.016	0.623 ± 0.002
B[1]	–80	45.6	38	1667 ± 160	4.93 ± 0.32	27.45 ± 12	0.267 ± 0.001	0.940 ± 0.018	1.079 ± 0.018	0.622 ± 0.001
B[1]	–80	88.9	38	1682 ± 161	4.99 ± 0.33	28.02 ± 12	0.266 ± 0.004	0.942 ± 0.021	1.077 ± 0.016	0.623 ± 0.001
B[1]	–25	57.1	93	1710 ± 164	5.74 ± 0.36	27.86 ± 12	0.268 ± 0.001	0.927 ± 0.011	1.087 ± 0.013	0.624 ± 0.001
B[1]	80	53.5	198	1745 ± 167	5.78 ± 0.46	30.74 ± 13	0.271 ± 0.001	0.886 ± 0.041	1.076 ± 0.021	0.627 ± 0.001
F[1]	–110	73.5	84	1688 ± 162	5.29 ± 0.34	28.35 ± 12	0.265 ± 0.001	0.933 ± 0.017	1.052 ± 0.023	0.623 ± 0.002
J[1]	–105	94.4	159	1749 ± 168	7.36 ± 0.47	28.85 ± 12	0.270 ± 0.001	0.912 ± 0.011	1.102 ± 0.012	0.627 ± 0.001
N[1]	–105	57.1	239	1768 ± 170	6.40 ± 0.43	31.01 ± 13	0.285 ± 0.003	0.908 ± 0.028	1.063 ± 0.017	0.633 ± 0.001
B	–25	72.0	93	2140 ± 255	6.16 ± 0.17	27.95 ± 2.00	0.272 ± 0.005	0.937 ± 0.031	1.075 ± 0.025	0.628 ± 0.004
B	–178	54.0	61	1743 ± 106	5.37 ± 0.32	25.71 ± 1.84	0.264 ± 0.003	0.929 ± 0.042	1.038 ± 0.029	0.625 ± 0.002
B	–293	72.7	176	1753 ± 162	5.75 ± 0.24	28.07 ± 2.00	0.280 ± 0.003	0.944 ± 0.029	1.079 ± 0.021	0.624 ± 0.001
B	–133	72.6	18	1744 ± 157	5.41 ± 0.19	25.38 ± 1.81	0.262 ± 0.004	0.922 ± 0.025	1.051 ± 0.036	0.621 ± 0.002
F	–165	63.0	96	1645 ± 114	5.19 ± 0.21	24.54 ± 1.75	0.265 ± 0.005	0.940 ± 0.030	1.082 ± 0.043	0.619 ± 0.003
J	–235	77.1	198	1691 ± 159	5.61 ± 0.17	26.07 ± 1.86	0.269 ± 0.003	0.990 ± 0.024	1.068 ± 0.027	0.629 ± 0.002
J	–105	94.1	159	1737 ± 225	8.22 ± 0.38	25.63 ± 1.00	0.269 ± 0.004	0.940 ± 0.033	1.130 ± 0.037	0.628 ± 0.006
B	–25	50.5	93	1732 ± 88	4.98 ± 0.29	19.01 ± 0.73	0.258 ± 0.002	0.955 ± 0.049	1.063 ± 0.051	0.624 ± 0.003
J	95	21.7	265	1784 ± 77	6.91 ± 0.53	28.15 ± 1.04	0.292 ± 0.003	0.960 ±0.053	1.084 ± 0.051	0.639 ± 0.004
B	5	58.4	123	1740 ± 127	5.40 ± 0.28	26.35 ± 0.97	0.268 ± 0.003	0.935 ± 0.030	1.049 ± 0.034	0.625 ± 0.003
N	–290	54.3	295	1960 ± 152	6.99 ± 0.37	29.96 ± 1.10	0.283 ± 0.003	0.950 ± 0.031	1.065 ± 0.037	0.636 ± 0.003
J	–40	71.7	177	1846 ± 185	6.05 ± 0.31	27.41 ± 1.01	0.276 ± 0.003	0.940 ± 0.028	1.050 ± 0.034	0.630 ± 0.003
F	–65	72.7	99	1776 ± 171	5.43 ± 0.29	25.56 ± 0.94	0.269 ± 0.003	0.926 ± 0.030	1.048 ± 0.035	0.624 ± 0.004
N	–5	74.4	264	1976 ± 233	7.29 ± 0.38	29.97 ± 1.12	0.291 ± 0.004	0.937 ± 0.032	1.052 ± 0.041	0.636 ± 0.005
F	–165	85.3	96	1800 ± 220	5.39 ± 0.27	25.59 ± 0.94	0.270 ± 0.004	0.931 ± 0.026	1.084 ± 0.030	0.624 ± 0.003
J	95	21.4	265	1626 ± 69	5.87 ± 0.47	28.74 ± 1.55	0.288 ± 0.002	0.944 ± 0.053	1.043 ± 0.049	0.639 ± 0.003
B	–178	93.0	61	1693 ± 214	5.07 ± 0.27	23.65 ± 0.88	0.268 ± 0.003	0.916 ± 0.031	1.050 ± 0.037	0.623 ± 0.004
B	–80	21.7	38	1734 ± 117	5.33 ± 0.26	25.81 ± 1.39	0.264 ± 0.003	0.926 ± 0.037	1.077 ± 0.042	0.618 ± 0.007

[1]Samples measured on the MAP 215–50.

Table 2. Helium, Ne, and Ar concentrations (in 10^{-8} cm^3 STP/g) for Carbo. Neon-21 is not corrected for S + P contributions.

Bar	Distance from ref. line (mm)	Mass (mg)	Distance from center (mm)	$^4He \pm 2\sigma$	$^{21}Ne \pm 2\sigma$	$^{38}Ar \pm 2\sigma$	$^3He/^4He \pm 2\sigma$	$^{20}Ne/^{21}Ne \pm 2\sigma$	$^{22}Ne/^{21}Ne \pm 2\sigma$	$^{36}Ar/^{38}Ar \pm 2\sigma$
				(10^{-8} cm^3 STP/g)						
Y	–115	95.2	434	1741 ± 266	5.22 ± 0.25	23.68 ± 1.03	0.263 ± 0.004	0.950 ± 0.029	1.079 ± 0.033	0.611 ± 0.004
V	–80	75.4	352	1512 ± 127	4.17 ± 0.18	19.75 ± 1.02	0.257 ± 0.003	0.912 ± 0.024	1.067 ± 0.027	0.623 ± 0.014
S	–40	101.4	266	1443 ± 186	3.83 ± 0.27	18.78 ± 0.85	0.254 ± 0.004	0.933 ± 0.036	1.048 ± 0.035	0.618 ± 0.007
P	18	89.2	171	1349 ± 127	4.02 ± 0.25	17.63 ± 0.88	0.248 ± 0.003	0.927 ± 0.025	1.109 ± 0.026	0.614 ± 0.013
M	35	100.4	105	1303 ± 139	3.25 ± 0.22	16.97 ± 0.83	0.249 ± 0.003	0.936 ± 0.036	1.051 ± 0.038	0.611 ± 0.012
J	41	92.9	81	1267 ± 118	3.19 ± 0.21	16.38 ± 0.76	0.249 ± 0.003	0.947 ± 0.030	1.071 ± 0.033	0.616 ± 0.008
J	3	83.3	118	1299 ± 108	3.48 ± 0.22	16.79 ± 0.94	0.245 ± 0.005	0.914 ± 0.029	1.068 ± 0.030	0.616 ± 0.018
J	–30	76.6	151	1314 ± 97	3.88 ± 0.25	17.51 ± 0.82	0.247 ± 0.003	0.918 ± 0.026	1.095 ± 0.032	0.607 ± 0.010
J	–88	82.6	209	1364 ± 119	3.50 ± 0.24	17.82 ± 0.95	0.251 ± 0.003	0.940 ± 0.032	1.075 ± 0.028	0.613 ± 0.014
J	–160	56.1	281	1463 ± 82	4.25 ± 0.29	20.33 ± 1.14	0.251 ± 0.003	0.893 ± 0.030	1.046 ± 0.048	0.619 ± 0.018
G	–33	92.7	178	1316 ± 130	3.41 ± 0.22	17.77 ± 0.85	0.251 ± 0.003	0.939 ± 0.030	1.055 ± 0.034	0.624 ± 0.011
D	–113	62.8	287	1496 ± 101	4.76 ± 0.36	20.03 ± 0.95	0.252 ± 0.003	0.919 ± 0.043	1.089 ± 0.049	0.612 ± 0.010
G	63	74.7	107	1278 ± 87	3.36 ± 0.22	16.83 ± 0.82	0.246 ± 0.003	0.939 ± 0.029	1.079 ± 0.037	0.615 ± 0.011
M	–7	62.2	141	1276 ± 68	3.42 ± 0.24	16.88 ± 0.78	0.247 ± 0.003	0.934 ± 0.041	1.066 ± 0.042	0.614 ± 0.008
A	36	84.2	257	1463 ± 147	3.81 ± 0.26	18.86 ± 0.84	0.252 ± 0.003	0.930 ± 0.035	1.069 ± 0.033	0.616 ± 0.006
A	–107	79.4	333	1027 ± 57	2.64 ± 0.19	13.02 ± 0.65	0.252 ± 0.003	0.911 ± 0.035	1.029 ± 0.039	0.619 ± 0.013
J	–160	92.7	281	1452 ± 172	4.25 ± 0.23	19.60 ± 0.95	0.255 ± 0.004	0.942 ± 0.026	1.076 ± 0.029	0.628 ± 0.010
J	–30	45.2	151	1270 ± 47	3.32 ± 0.18	17.82 ± 0.83	0.246 ± 0.002	0.945 ± 0.029	1.040 ± 0.039	0.608 ± 0.010
M	–7	56.7	141	1256 ± 59	3.41 ± 0.22	16.82 ± 0.74	0.245 ± 0.002	0.933 ± 0.037	1.089 ± 0.040	0.607 ± 0.004
Y	–115	101.7	434	1750 ± 335	5.54 ± 0.28	24.11 ± 1.20	0.263 ± 0.005	0.920 ± 0.023	1.069 ± 0.035	0.623 ± 0.012
V	–80	66.1	352	1538 ± 119	4.39 ± 0.22	20.91 ± 1.27	0.254 ± 0.003	0.922 ± 0.021	1.043 ± 0.037	0.629 ± 0.021
D	–113	80.8	287	1494 ± 149	4.22 ± 0.26	19.95 ± 0.92	0.253 ± 0.003	0.928 ± 0.032	1.055 ± 0.026	0.609 ± 0.008
A	–175	66.3	382	1614 ± 135	5.27 ± 0.27	21.41 ± 0.97	0.259 ± 0.003	0.930 ± 0.025	1.091 ± 0.038	0.621 ± 0.007
S	–40	102.4	266	1381 ± 156	3.70 ± 0.17	16.49 ± 0.75	0.244 ± 0.004	0.961 ± 0.033	1.035 ± 0.038	0.615 ± 0.013
M	35	84.9	105	1335 ± 108	4.37 ± 0.23	16.03 ± 0.61	0.245 ± 0.003	0.895 ± 0.036	1.108 ± 0.047	0.608 ± 0.003
G	63	64.1	107	1292 ± 67	3.55 ± 0.22	16.13 ± 0.61	0.240 ± 0.003	0.923 ± 0.047	1.065 ± 0.061	0.606 ± 0.003
P	18	83.7	171	1331± 105	3.76 ± 0.18	16.82 ± 0.64	0.244 ± 0.003	0.901 ± 0.033	1.103 ± 0.039	0.607 ± 0.004
G	–33	99.7	178	1373 ± 148	3.73 ± 0.18	16.42 ± 0.62	0.247 ± 0.003	0.943 ± 0.038	1.083 ± 0.045	0.606 ± 0.003
J	41	112.2	81	1265 ± 142	3.71 ± 0.13	16.08 ± 0.63	0.247 ± 0.003	0.916 ± 0.025	1.075 ± 0.036	0.607 ± 0.006
A	–175	67.3	382	1679 ± 139	4.94 ± 0.23	23.77 ± 0.97	0.250 ± 0.004	0.929 ± 0.031	1.084 ± 0.033	0.613 ± 0.009
J	–88	95.6	209	1387 ± 145	3.85 ± 0.16	17.19 ± 0.75	0.251 ± 0.003	0.930 ± 0.031	1.066 ± 0.038	0.614 ± 0.010

corrections are smaller because the gas amounts used for calibrations fits rather well the typical sample gas amounts. For a typical sample the sensitivity increases by ~2% and 3% for Ne and Ar, respectively.

Data Reduction

Besides mass fractionation the samples are also corrected for interferences and blanks. For the MAP spectrometer the mass resolution is sufficient to resolve HD from ^{3}He and $H_2{}^{18}O$ from ^{20}Ne, therefore no corrections are needed. Even if the double-to-single charged ratio for ^{40}Ar is fairly large ($^{40}Ar^{++}/^{40}Ar^{+} = 0.67$), the corrections for doubly charged ^{40}Ar on ^{20}Ne usually are very small. For a typical sample $^{40}Ar^{++}$ contributes less than 1% to ^{20}Ne. Carbon dioxide has a double to single charged ratio of 0.01 and $CO_2{}^{++}$ contributes less than 0.05% to ^{22}Ne. For the system B spectrometers the H_2, H_2O, CO_2, and ^{40}Ar amounts are comparable for sample and blank measurements, thus corrections were made via the blank correction.

Procedure blanks are very minor. They usually contribute less than ~3‰ for ^{4}He, ^{20}Ne, and ^{36}Ar. Since all samples clearly show cosmogenic noble gas ratios ($^{20}Ne/^{22}Ne \approx 0.93$, $^{36}Ar/^{38}Ar \approx 0.63$), no correction for trapped noble gases was necessary.

Uncertainties

The uncertainties given in Tables 1 and 2 are 2σ and include the statistical uncertainties of the measurements, blank corrections, interference corrections, corrections for sensitivity changes, and fractionation. Due to technical problems the calibration of the MAP spectrometer had to be re-adjusted using well studied meteorites, i.e., the L-chondrite Bruderheim (Zurich-Standard) and the eucrite Millbillillie, and a new air standard. The recalibration increased the uncertainty (1σ) for the measured He, Ne, and Ar concentrations to ~5%, ~3%, and ~20%, respectively. Note that the recalibration only affects the measurements performed on the MAP spectrometer and does not concern the majority of our measurements, which were performed on the system B spectrometers.

Since the recalibration procedure does not affect isotopic ratios, their uncertainties (1σ) are similar for both systems (MAP, system B), i.e., $^{3}He/^{4}He$: 0.6%, Ne-ratios: 2%, $^{36}Ar/^{38}Ar$: 0.5%. For the system B spectrometers, the correction for non-linearities, i.e., the dependence of sensitivity and mass discrimination on gas amounts significantly increases the uncertainties, whereas the He data are most affected. For example, the non-linearities add a 1σ uncertainty between 2% and 7% to the given ^{4}He concentrations for samples with masses between 20 mg and 100 mg. The additional uncertainties for Ne and Ar are much lower, i.e., 3% and 2%, respectively. However, when comparing noble gas data of different laboratories, additional uncertainties of 5% for concentrations and 1% for isotopic ratios have to be taken into account (Michel et al. 1989).

RESULTS

Noble Gas Data

Tables 1 and 2 give the measured cosmogenic noble gas concentrations and isotopic ratios for He, Ne, and Ar for Grant and Carbo together with the sample locations. The He and Ar concentrations for replicate analysis of samples from same locations within the meteoroids usually agree within 2σ and the different profiles show a consistent pattern. The scatter for Ne isotopic concentrations is significantly larger than the scatter observed for He and Ar concentrations and often exceeds the 2σ uncertainties (see Figs. 4a, 4b and 7a, 7b).

For one sample (Carbo A-107), the gas amounts are surprisingly low in all He, Ne, and Ar concentrations, which might be attributed to an incorrect sample weight or incomplete sample degassing. A high ^{4}He concentration, i.e., ~25% higher than in the other aliquots of the same sample, was measured in one aliquot of Grant B-25. However, so far we have no explanation for the observed discrepancy. Note that the third aliquot of B-25 has insufficient amounts of Ne (~15%) and Ar (~45%), which most probably indicates an incomplete degassing.

In general, our new data agree well with results published earlier for Grant (Signer and Nier 1960, 1962; Graf et al. 1987) and Carbo (Hoffman and Nier 1959). Therefore, for both meteorites there now exists a consistent and well-proven database for cosmogenic He, Ne, and Ar isotope concentrations for samples with known locations within the parent body. Such a database is mandatory for detailed studies of cosmogenic production systematics in iron meteorites.

SEM Analyses

We studied samples from Grant and Carbo using a Cam Scan CS4 scanning electron microscope (SEM) equipped with a Voyager EDX-System to analyze the chemistry of the metal ground phase in general and to get an idea of the presence of microscopic mineral inclusions. The chemical composition of the sample is of major importance for the study of cosmogenic production systematics because different elements have different cosmogenic production rates. Figures 2a and 2b show backscattered electron images of Grant (J-105) and Carbo (V-80), respectively. The Ni-rich (lighter) taenite can be clearly distinguished from the Ni-poor (darker) kamacite. It can also be seen that the Ni content decreases towards the center of the taenite lamellae as described, e.g., by Mittlefehldt et al. (1998). In Grant, 2 different types of inclusions can be seen: first, the dark

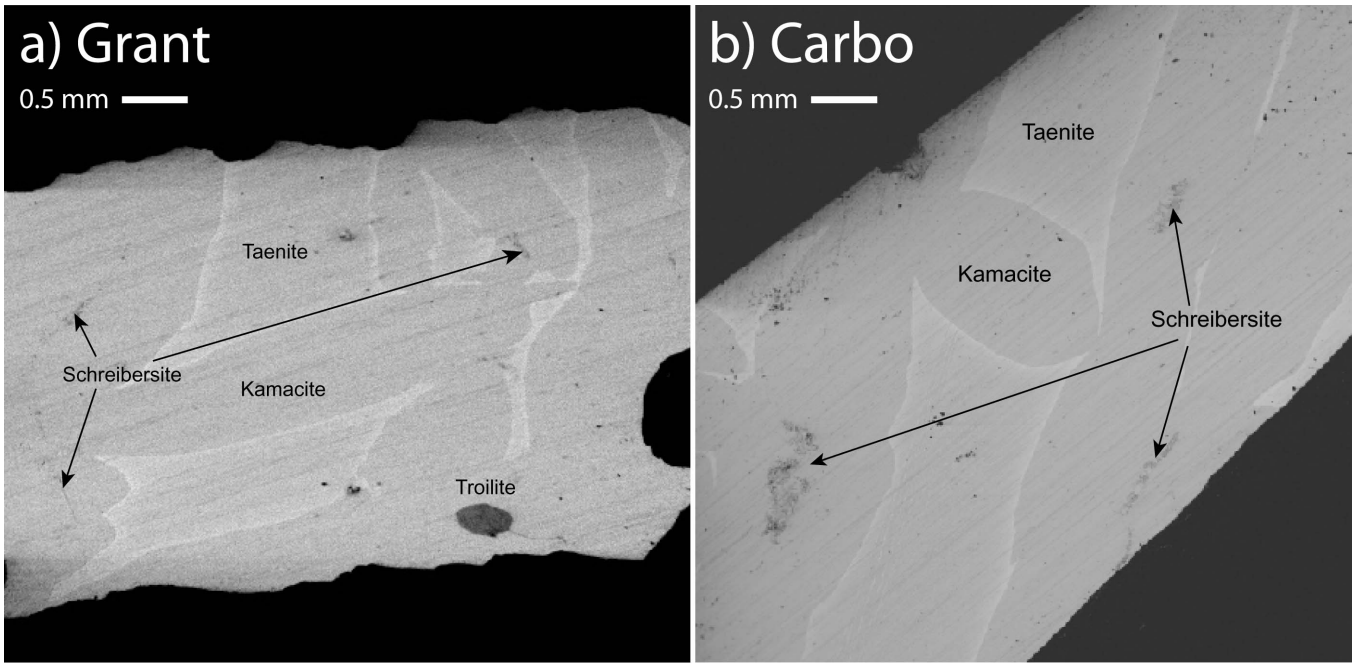

Fig. 2. Backscatter images of Grant (J-105, panel a) and Carbo (V-80, panel b). On both images kamacite (Ni-poor, dark area) and taenite (Ni-rich, lighter area) can be clearly distinguished. Two different types of inclusions are visible: troilite (dark nodule) and schreibersite (elongates and skeletal shape).

rounded nodule, which is troilite, and second the lighter, skeletal one, which is schreibersite. In the Carbo sample only schreibersite inclusions are visible. As described by Buchwald (1975, p. 472 for Carbo and p. 613 for Grant) troilite and schreibersite are very common in these 2 meteorites. Beside the big inclusions (up to 25–50 mm across) there are also a lot of smaller inclusions with sizes of 5–400 μm for schreibersite and 5 μm to 2 mm for troilite, respectively.

DISCUSSION

New Preatmospheric Center Locations for Grant and Carbo

For determining the preatmospheric centers of Grant and Carbo we used so-called "contour plots" in which lines represent locations of identical gas concentrations or isotopic/elemental ratios. They are based on the observation that (in iron meteorites) noble gas concentrations as well as isotopic and elemental ratios are one-to-one functions of shielding depth (e.g., Wieler 2002; Leya et al. 2004). Figs. 3a and 3b show contour plots of ^{38}Ar concentrations for Carbo and ^{4}He/^{21}Ne ratios for Grant. Considering also the 3rd dimension, contour lines represent shells of equal irradiation conditions (similar particle spectra and flux densities). Consequently, gradients perpendicular to the contour-shells (or contour lines in 2D) point towards the preatmospheric center. Contour plots of ^{4}He, ^{20}Ne, ^{21}Ne, ^{22}Ne, ^{36}Ar, ^{36}Ar/^{38}Ar, and ^{4}He/^{21}Ne indicate a consistent center location for Grant at 117 mm left of the reference line and 9 mm below bar B (Fig. 3b). All individual center locations agree within a 1σ uncertainty of ~15 mm. The new preatmospheric center location agrees well with earlier estimates by Leya (1997, p. 346) but is significantly different (~10 cm) from the center location originally determined by Signer and Nier (1960) at ~165 mm left from the reference line on bar F (see Fig. 3b). The same procedure was used for Carbo which results in an average center location of 120 mm right of the reference line and 15 mm above bar J. The 1σ uncertainty is ~25 mm (Fig. 3a). The new preatmospheric center location is in good agreement with an earlier estimate by Hoffmann and Nier (1959). A correct preatmospheric center location is mandatory to investigate the depth dependencies for production rates of cosmogenic nuclides in iron meteorites. These data are of major importance for the evaluation of the upcoming model calculations.

We want to emphasize that the procedure described above is based on stable isotopes only and therefore gives a "mean" center location, i.e., the center location valid for most of the lifetime of the meteoroid. For example, a breakup a few million years before entering the Earth's atmosphere would not be detectable by this procedure because such an event would cause only a very minor change in the noble-gas distribution.

Exposure Histories

Using cosmogenic radionuclides it is possible to detect a complex exposure history of a meteoroid. Radionuclides only record information about the exposure conditions over a few

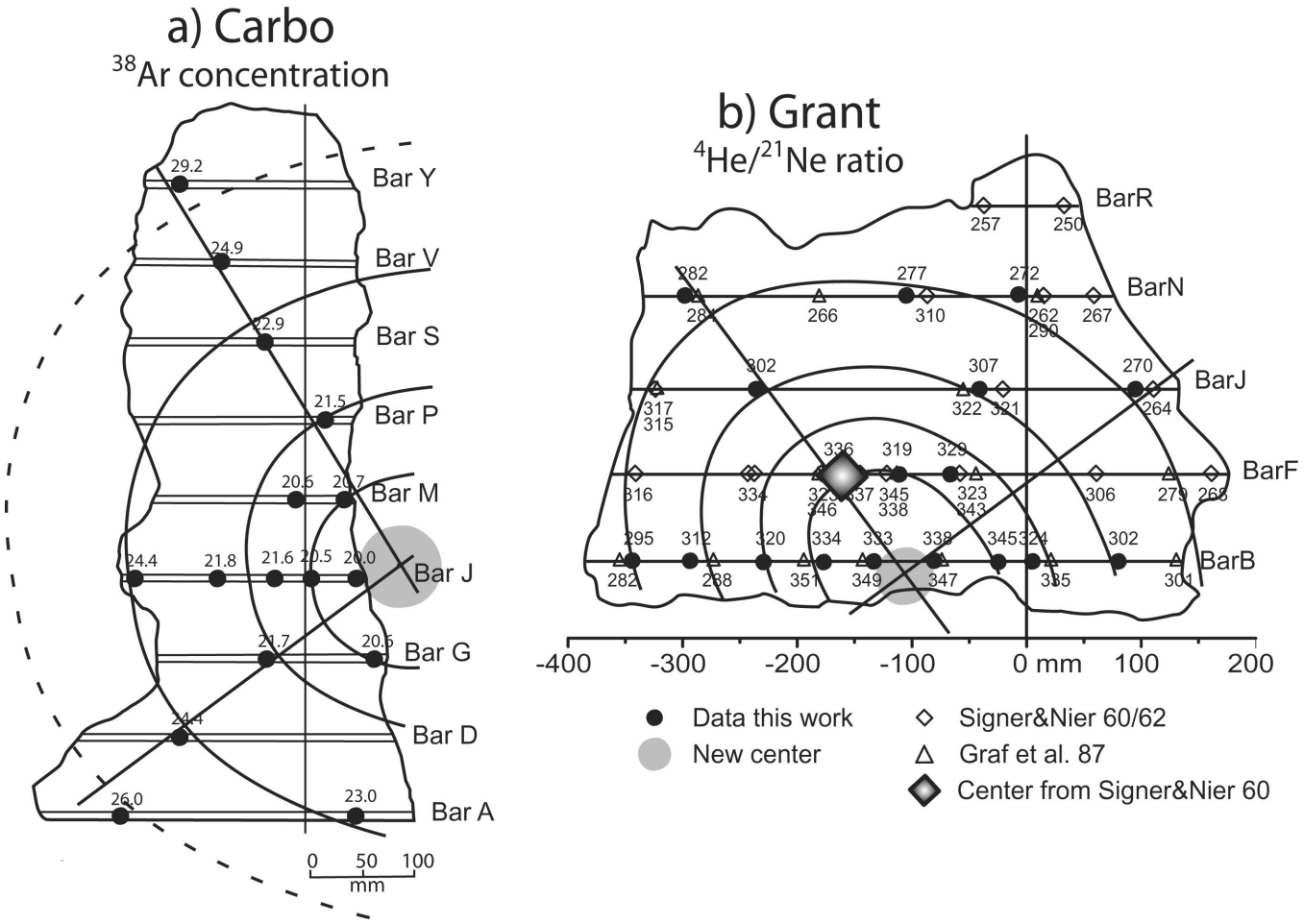

Fig. 3. Argon-38 contour plot for Carbo (a) and $^{4}He/^{21}Ne$ contour plot for Grant (b). The shaded circles show the preatmospheric center locations, whereas their radius corresponds to the 2σ uncertainties, which is ~45 mm and ~30 mm for Carbo and Grant, respectively.

half-lives. A discrepancy between the center location determined from radionuclides and stable noble gas nuclides would thus unambiguously indicate a complex exposure of the studied meteorite. The radionuclide ^{10}Be is particularly well suited for such studies as it shows a strong depth dependency. From literature ^{10}Be data (Graf et al. 1987; Xue et al. 1995) we determined a preatmospheric center location for Grant at 137 mm left of the reference line on bar B. This location agrees well with the one determined from noble gases, thus a complex exposure for Grant is unlikely (see also Lavielle et al. 1999). For Carbo only few radionuclide data with badly documented sample locations were found in literature, which prevents a definitive conclusion.

Preatmospheric Geometries

With the new preatmospheric center locations for Grant and Carbo and assuming a simple exposure, it is possible to determine the geometry of both meteoroids by arranging our data in so-called depth-profiles, i.e., concentrations and ratios as a function of the distance from the center. For a spherical object every point at the same distance from the center should have the same gas concentration and isotopic/elemental ratio. Figures 4a and 4b show measured ^{4}He concentrations of the different depth-profiles measured in Grant and Carbo, respectively. All profiles agree within their uncertainties, indicating a circular shape of the meteoroids in the 2 dimensions studied. Although we have no information about the third dimension we consider it rather unlikely that Grant and Carbo were extremely elongated in that direction, because the probability of having cut the meteorites exactly perpendicular to this axis is fairly low. Therefore, we assume that Grant and Carbo were spherical objects for most of their lifetimes.

Preatmospheric Radii

For a cosmogenic radionuclide in saturation the measured activity equals the production rate, which depends only on the size of the meteoroid, the shielding depth, and the chemistry of the studied sample. Therefore, radionuclides can be used to determine the preatmospheric radius of a

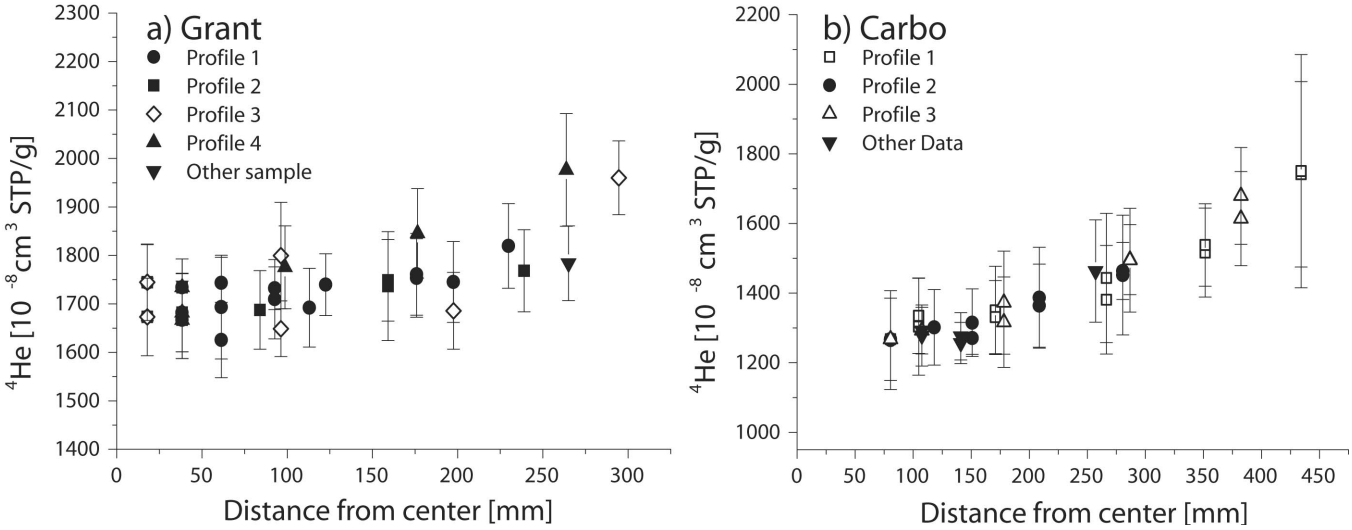

Fig. 4. Concentration of cosmogenic ^{4}He for Grant (a) and Carbo (b). The samples are distinguished according to the different directions along the center slice. The ^{4}He concentrations agree well within their 2σ uncertainties, giving a consistent depth profile. Therefore, the preatmospheric shapes of both meteorites are approximately spherical (at least in the 2 dimensions studied). From this result we also argue that both meteorites were spherical objects most of their lifetime in space (see text).

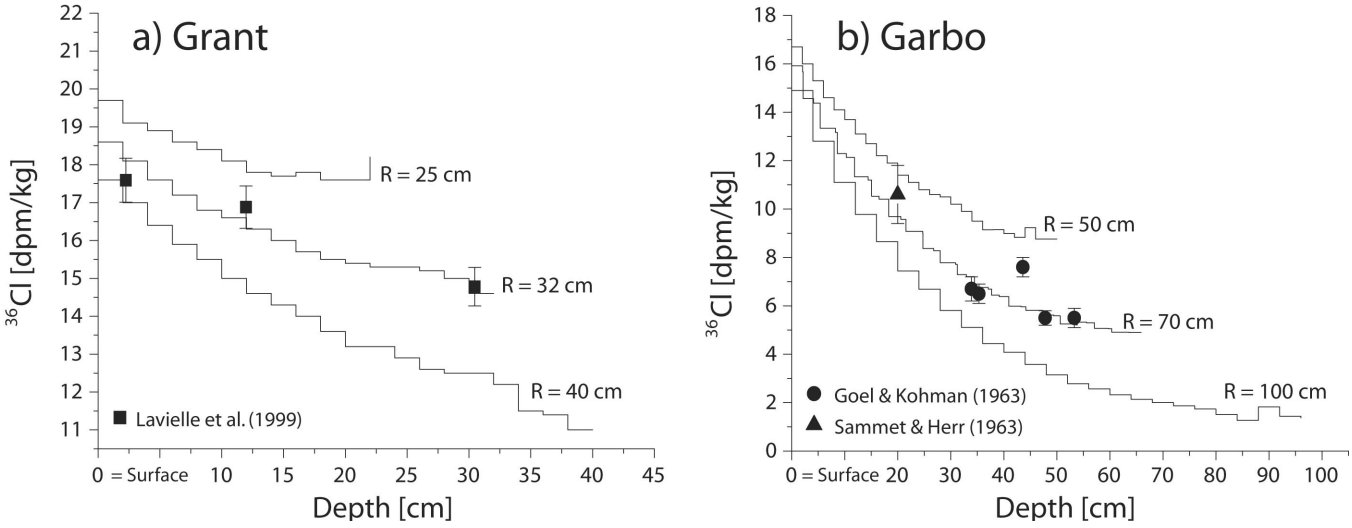

Fig. 5. Comparison of modeled and measured ^{36}Cl depth profiles assuming radii of 25–40 cm for Grant (a) and 50–100 cm for Carbo (b). The measured ^{36}Cl activities indicate a preatmospheric radius of ~32 cm for Grant and ~70 cm for Carbo.

meteoroid if the center location and sample positions are known. To do so we compared measured literature ^{36}Cl depth profiles of Grant and Carbo with modeled ones (Figs. 5a, 5b). A detailed description of the model and further model predictions for other cosmogenic nuclides will be given elsewhere. We focus here on ^{36}Cl, as its production rate is only marginally affected by target elements other than Fe and Ni and is therefore not compromised by inhomogeneous target element distribution. Experimental ^{36}Cl data for Grant are from Lavielle et al. (1999); for Carbo we used data the from Goel and Kohmann (1963) and Sammet and Herr (1963). Figures 5a and 5b demonstrate that the best agreement between modeled and measured data is for a preatmospheric radius of ~32 cm for Grant and ~70 cm for Carbo.

Mineral Inclusions and Their Influence on Cosmogenic Production Rates

Beside the major elements (Fe and Ni) iron meteorites also contain other elements like S, P, and C, which can influence the production rates for cosmogenic nuclides. The most common mineral inclusions are troilite (FeS), schreibersite ((Fe,Ni)$_3$P), and graphite (C) (Mittlefehldt et al. 1998). The production of cosmogenic Ne from S is more than an order of magnitude higher compared to production from Fe or Ni (Begemann 1965; Levsky and Komarov 1974; Leya et al. 2004). Consequently, in a Fe-Ni sample even 0.5% of S increases the cosmogenic ^{21}Ne concentration by about 20%, an effect which has to be considered when studying iron

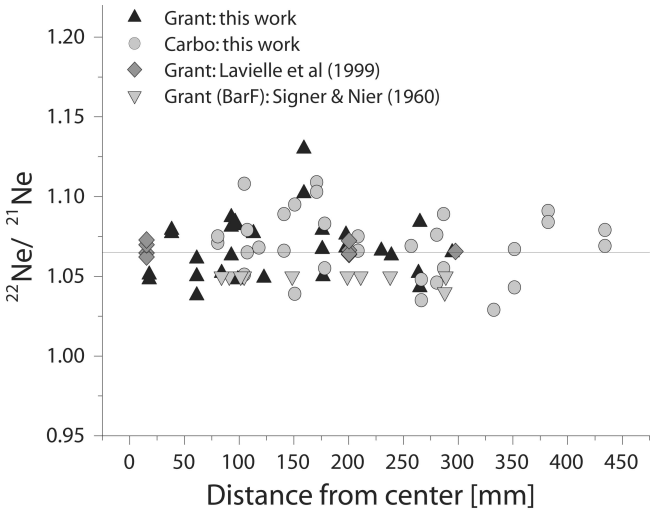

Fig. 6. Cosmogenic $^{22}Ne/^{21}Ne$ ratios as a function of the distance from the preatmospheric center for Grant and Carbo. The data clearly indicate that the cosmogenic $^{22}Ne/^{21}Ne$ ratios show no dependence on the shielding depth.

meteorites. The production rates of cosmogenic Ne from P are poorly constraint. However, since P and S have similar mass numbers, we expect similar Ne production rates for both elements.

Considering that a typical sample for our noble gas analysis has a volume of about 8–12 mm^3 (50–100 mg), troilite and schreibersite inclusions with grain sizes of a few hundred microns can easily be overlooked during sample preparation. Still, such small inclusions are big enough to significantly increase the production of cosmogenic Ne (see the Assumptions section). Since we observed a correlation between high Ne concentrations and the $^{22}Ne/^{21}Ne$ ratios in our samples, we suggest that it could be possible to correct the data for S and P contributions.

NEON-21 CORRECTION FOR S- AND P-RICH INCLUSIONS

Assumptions

The average $^{22}Ne/^{21}Ne$ ratio for meteoritic metal (93% Fe and 7% Ni) is deduced from recent measurements of artificially irradiated Fe and Ni foils (thin samples) is 1.02 ± 0.13 (Ammon et al. 2008). Experimental data from Leya et al. (2004) from thick target simulation experiments give a $^{22}Ne/^{21}Ne$ ratio for Fe and Ni of 1.04 ± 0.04, i.e., within the error identical to the data obtained from the thin targets. In contrast, an average $^{22}Ne/^{21}Ne$ ratio of 1.21 ± 0.04 has been calculated for troilites from 6 different iron meteorites (Begemann 1965; Alexander et al. 1968; Fireman and De Felice 1968; Schlotz 1977). For schreibersite a ratio of 1.19 ± 0.01 has been obtained using 2 different iron meteorites (Begemann 1965; Levsky and Komarov 1974). The finding that mineral inclusions and pure metal have significantly different $^{22}Ne/^{21}Ne$ ratios enables to quantify (and correct for) the amount of Ne produced in such mineral inclusions. However, the procedure developed by us does not allow distinguishing between contributions from troilite and schreibersite. Therefore, for quantifying their contributions to the total Ne amount only two $^{22}Ne/^{21}Ne$ endmember ratios have to be known, one for pure S + P and one for a typical meteoritic mixture of Fe + Ni.

Now the question is whether our procedure, i.e., the input data, depends on the size of the meteorites and the shielding depths of the studied samples or whether it is possible to establish a size and shielding independent approach. The $^{22}Ne/^{21}Ne$ ratio in iron meteorites does not depend on the size of the meteoroid and the shielding depth of the sample (see Fig. 6), which is also confirmed by the data from irradiated thin and thick targets. Therefore, we can conclude that the endmember ratios $(^{22}Ne/^{21}Ne)_{Fe+Ni}$ and $(^{22}Ne/^{21}Ne)_{S+P}$ are strictly valid, independent of the size and shielding conditions. However, preliminary model calculations suggest that the production rate ratio Ne_{S+P}/Ne_{Fe+Ni}, which is another important input-parameter in our approach, increases with increasing radius and sample depth. However, this effect does not affect the results (or has only a minor influence). Since the $^{22}Ne/^{21}Ne$ endmember ratios for S and P are rather well defined using troilite and schreibersite data, the quality of our approach to quantify the contributions from S- and P-rich inclusions to the total Ne amount in iron meteorites crucially depends on the $^{22}Ne/^{21}Ne$ endmember ratio for pure meteoritic metal, i.e., without any inclusions, for which no experimental data exist. An upper limit for the $(^{22}Ne/^{21}Ne)_{Fe+Ni}$ ratio is given by the experimental data from Grant and Carbo. For example, assuming $(^{22}Ne/^{21}Ne)_{Fe+Ni} > 1.05$, more than one third of our samples would have $^{22}Ne/^{21}Ne$ ratios below the limit for pure Fe + Ni, which then could not be understood. A lower limit for the $(^{22}Ne/^{21}Ne)_{Fe+Ni}$ endmember is given by the finding that a too low ratio results in (numerically, according to our correction) depth dependent contributions from S and P, which is unrealistic. This limits the $(^{22}Ne/^{21}Ne)_{Fe+Ni}$ ratio to values larger than 1.02. For the final correction we use a value of 1.03 ± 0.02, which is the average of the experimental data from thin and thick targets (Leya et al. 2004; Ammon et al. 2008) and which is well within the limits defined above. With the thus determined $(^{22}Ne/^{21}Ne)_{Fe+Ni}$ ratio and production rate ratios Ne_{S+P}/Ne_{Fe+Ni} between 30–60 (which are average values for Grant and Carbo) we obtain a $^{22}Ne/^{21}Ne$ endmember ratio for pure S and P of 1.214 ± 0.004.

Correction of Neon from Sulphur and Phosphorus

The measured Ne_m consists of Ne produced from Fe and Ni (Ne_{Fe+Ni}), and of Ne produced from S and P (Ne_{S+P}). Therefore, Ne_{S+P} is given by:

$$^{20,21,22}Ne_{S+P} = {}^{20,21,22}Ne_{m} - {}^{20,21,22}Ne_{Fe+Ni} \quad (1)$$

The measured $^{22}Ne/^{21}Ne$ ratio R_M varies with the contributions from S and P in the sample. Since the concentration of Ne_{Fe+Ni} with a $^{22}Ne/^{21}Ne$ ratio of $R_{Fe} = 1.030$ and Ne_{S+P} with a $^{22}Ne/^{21}Ne$ ratio of $R_S = 1.214$ is not known we have to modify Equation 1:

$$\frac{^{22}Ne_{S+P}}{^{21}Ne_{S+P}} = R_S = \frac{^{22}Ne_m - {}^{22}Ne_{Fe+Ni}}{^{21}Ne_m - {}^{21}Ne_{Fe+Ni}} \quad (2)$$

With $^{22}Ne_m = {}^{21}Ne_m \times R_M$ and $^{22}Ne_{Fe+Ni} = {}^{21}Ne_{Fe+Ni} \times R_{Fe}$ we can write:

$$R_S = \frac{R_M \times {}^{21}Ne_m - R_{Fe} \times {}^{21}Ne_{Fe+Ni}}{^{21}Ne_m - {}^{21}Ne_{Fe+Ni}} \quad (3)$$

Thus, cosmogenic ^{21}Ne concentrations corrected for contributions from S and/or P are given by:

$$^{21}Ne_{Fe+Ni} = {}^{21}Ne_{corr} = \frac{R_M - R_S}{R_{Fe} - R_S} \times {}^{21}Ne_m \quad (4)$$

For the correction procedure assumptions are made only for the $^{22}Ne/^{21}Ne$ ratios of Fe + Ni (R_{Fe}) and S + P (R_S). Consequently, the uncertainties introduced by the corrections are dominated by the R_{Fe}, and hence the calculated R_S values, and are therefore hard to estimate. However, by varying the input parameters within reasonable limits we estimated an average uncertainty for the correction of about 10%.

Corrected ^{21}Ne for Grant and Carbo

Figures 7a and 7b show corrected (solid symbols) and uncorrected (open symbols) ^{21}Ne concentrations for Grant and Carbo, respectively. Both figures clearly demonstrate that the corrections are significant, e.g., for one Grant sample up to ~55% of the total measured ^{21}Ne has been produced from S and P. On average, ~20% of the total ^{21}Ne is produced from S and/or P and only ~80% is produced from Fe and Ni. The correction also allows conclusions about the contribution of S + P in a given sample. The average $^{22}Ne/^{21}Ne$ ratio of ~1.07 corresponds to the presence of about 0.5 wt.% S + P in a typical sample of Grant and Carbo and therefore about 1–2 vol% of troilite and schreibersite inclusions (which corresponds to an inclusion of ~0.11 mm^3 in a 8 mm^3 sample). This value seems to be realistic, since Mittlefehldt et al. (1998) give a range of 1.4–6% S and 0.6–1% P for IIIAB iron meteorites (e.g., Grant), including also visible inclusions. The P content in IID iron meteorites (e.g., Carbo) is also about 1%. Unfortunately Mittlefehldt et al. (1998) do not report any data for the S content of IID irons but according to Buchwald (1977) the S content of iron meteorites generally ranges from 0.02–12%. However, as a result of our correction procedure outliers are significantly reduced and now fit well into the overall systematics of the depth profile for Grant and Carbo (Figs. 7a and 7b).

THE INFLUENCE OF THE ^{21}Ne CORRECTION ON THE $^{41}K/^{40}K$ EXPOSURE AGES

We have demonstrated above that ^{21}Ne contributions from S- and/or P-rich inclusions are significant in Grant and Carbo. However, these contributions can be reliably quantified, which is of major importance for, e.g., the ^{41}K-^{40}K dating method. This method is widely used to determine cosmic-ray exposure ages for iron meteorites and it is based, among others, on measured $^{4}He/^{21}Ne$ ratios. According to our new results the ^{21}Ne concentrations have to be corrected. The ^{4}He production rates, on the other hand, depend only minimally on the chemical composition of the meteoroid (Leya et al. 2004), therefore no corrections for ^{4}He are applied.

Here we will briefly summarize the ^{41}K-^{40}K system developed by Voshage and co-workers (e.g., Voshage and Hintenberger 1961; Voshage 1967; Voshage and Feldmann 1979). According to these authors, the experimental results of the potassium isotopic measurements are summarized as parameter M:

$$M = \frac{^{41}K}{^{40}K} - a\frac{^{39}K}{^{40}K} \quad (5)$$

The parameter a is the isotopic ratio of terrestrial potassium $(^{41}K/^{39}K)_{norm}$. The production rates are summarized as parameter N accordingly:

$$N = \frac{P_{41}}{P_{40}} - a\frac{P_{39}}{P_{40}} \quad (6)$$

Since the long-lived ^{40}K ($T_{1/2} = 1.28$ Ga) is not in saturation, its production rate cannot be measured directly (Voshage 1962). To overcome this problem, Voshage (1978) studied ^{38}Ar, ^{39}Ar, and ^{36}Cl concentrations in 3 different iron meteorites and assumed a similar behavior for the co-produced potassium isotopes. Most importantly, he found, as expected, that the production rates of potassium isotopes depend on the size of the meteoroid and the shielding depth of the studied sample. To correct for this effect, the shielding parameter $^{4}He/^{21}Ne$ was introduced. The N value therefore cannot be determined directly and will be approximated as a function of the shielding parameter $^{4}He/^{21}Ne$:

$$N = 1.346 + 0.000515 \times {}^{4}He/^{21}Ne \quad (7)$$

We want to emphasize that Equation 7 has been determined by combining modeled production rates for He and Ne performed by Arnold et al. (1961), which only consider Fe and Ni as target elements, and experimental He and Ne data, which were measured by Schultz and Hintenberger (1967). For the latter, ^{21}Ne contributions from S- and/or P-rich inclusions

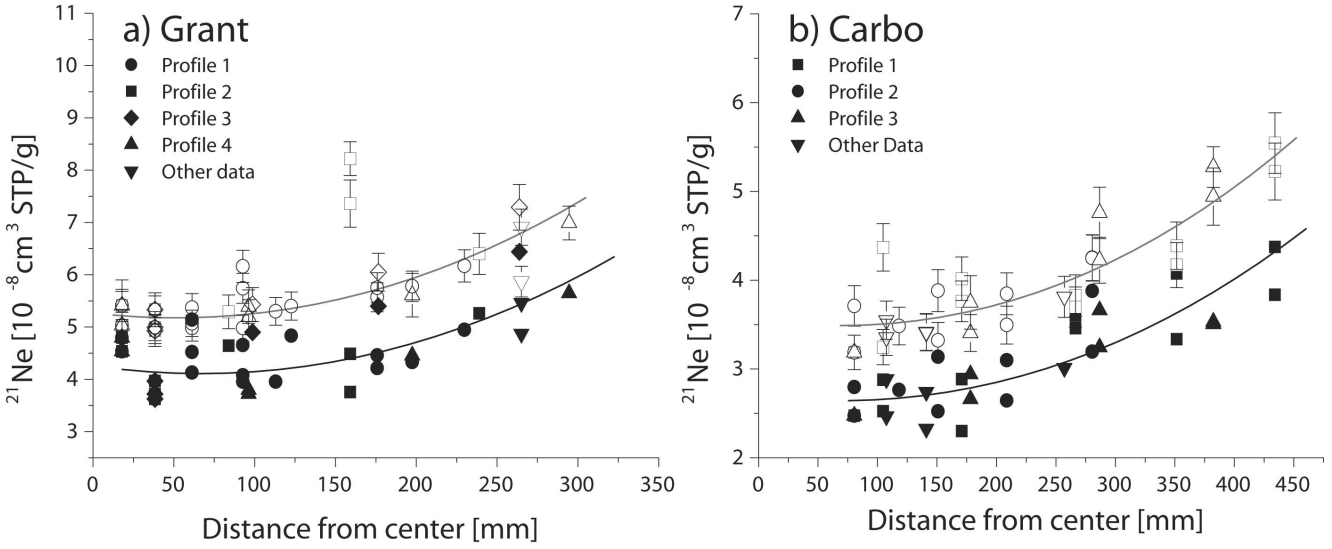

Fig. 7. Uncorrected (open symbols) and corrected (solid symbols) ^{21}Ne depth profiles for Grant (a) and Carbo (b). Correcting contributions from S- and P-rich inclusions eliminates outliers (Grant) and reduces the scattering (Carbo). The uncorrected data (open symbols) have an average 2σ uncertainty of 6%.

are significant but such contributions have not been considered while deducing Equation 7. Consequently, some inconsistencies exist when going from Equation 6 to Equation 7. While the model predictions only consider Fe and Ni as target elements, the experimental data used to adjust the model, are compromised by contributions from S and P. To obtain a consistent approach we corrected the ^{21}Ne data from Schultz and Hintenberger (1967) for contributions from S- and/or P-rich inclusions as described above. The new approximation of the N values (Equation 8) only considers ^{21}Ne which was produced by Fe and Ni. Therefore all input data to calculate exposure ages should be corrected accordingly using slightly revised N values.

$$N = 1.345 + 0.000527 \times (^4\mathrm{He}/^{21}\mathrm{Ne})_{corr} \quad (8)$$

Based on the M and N values the ^{41}K-^{40}K exposure ages T_K can be calculated via:

$$\frac{\lambda T_K}{\left(1 - e^{-\lambda T_K}\right)} = \frac{M}{N} \quad (9)$$

Where $\lambda = 0.5476 \times 10^{-9}$ is the decay constant of ^{40}K (latest value by Kwon et al. 2002) and T_K is the exposure age of the meteorite. Because Equation 9 cannot be solved analytically it has to be rearranged to determine exposure ages:

$$N = \frac{M \times \left(1 - e^{-\lambda T_K}\right)}{\lambda T_K} \quad (10)$$

Using M values for Grant and Carbo published by Voshage and Feldmann (1979), we can determine corresponding N values for exposure ages between 100 Ma and 1400 Ma. The exposure age T_K can then be plotted as a function of N (see Figs. 8a and 8b for Grant and Carbo, respectively). Using corrected ^{21}Ne concentrations new N values are obtained for Grant and Carbo and new cosmic-ray exposure ages can be deduced from Figs. 8a and 8b, respectively.

Note that the N value is a proxy for the K-production rate ratios and is therefore depth dependent as expressed by the dependence on the ^{4}He/^{21}Ne ratio. Consequently, for determining an exposure age, the M and N values have to be determined on the same sample or at least on samples with the same shielding conditions. Unfortunately, Voshage and Feldmann (1979) give no information for the ^{22}Ne/^{21}Ne ratios of the samples they studied. To calculate new exposure ages for Grant and Carbo using literature M values (Voshage and Feldmann 1979), we therefore used our samples (all aliquots) with uncorrected ^{4}He/^{21}Ne ratio similar to those measured by Voshage and Feldmann (1979). Using our uncorrected samples with an average ^{4}He/^{21}Ne ratio of 322, i.e., close to the ratio of the samples studied by Voshage and Feldmann (1979), results in an exposure age of 684 ± 63 Ma for Grant, which is, as expected, identical within uncertainties to the age of 695 ± 65 Ma given by Voshage and Feldmann (1979). However, if we correct ^{21}Ne for contributions from S- and/or P-rich inclusions, the average ^{4}He/^{21}Ne ratio increases from 322 to 413, which gives an exposure age of 564 ± 78 Ma. The corrected age is now closer to the ^{36}Cl-^{36}Ar-, ^{26}Al-^{21}Ne-, and ^{10}Be-^{21}Ne ages of 447 ± 9, Ma 500 ± 17 Ma, and 484 ± 12 Ma, respectively (Lavielle et al. 1999). The new cosmic-ray exposure age for Carbo of 725 ± 100 Ma is also lower than the value of 850 ± 140 Ma given by Voshage and Feldmann (1979). For this meteorite, unfortunately, the literature data are highly variable, e.g., published ^{36}Cl-^{36}Ar ages are 350 ± 40 (Sammet and Herr 1963) 720 ± 50 (Vilcsek and Wänke

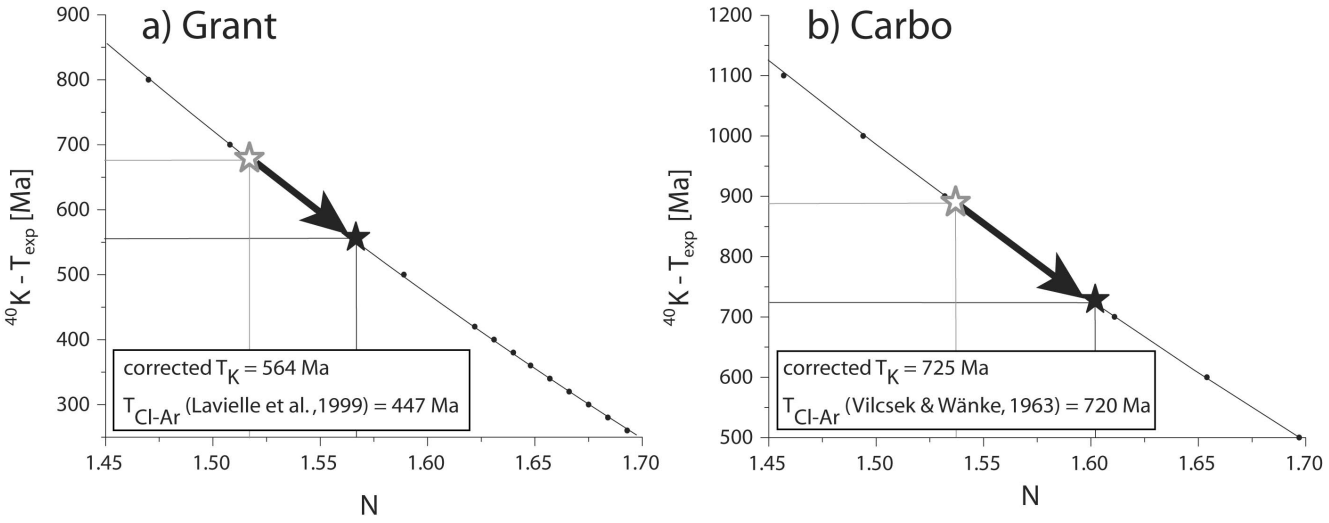

Fig. 8. ^{40}K-T$_{exp}$/N plot for Grant (a) and Carbo (b). Such a plot enables to precisely determine the cosmic-ray exposure ages using the ^{41}K/^{40}K-^{4}He/^{21}Ne dating system. Correcting contributions from S- and P-rich inclusions always increases the N value and therefore results in lower cosmic-ray exposure ages.

Table 3. M values, corrected and uncorrected ^{4}He/^{21}Ne ratios, and corrected and uncorrected cosmic-ray exposure ages for Grant and Carbo samples (and their replicates) with similar uncorrected ^{4}He/^{21}Ne ratios as given by Voshage and co-workers.

Meteorite	Sample	M	^{4}He/^{21}Ne uncorrected	T$_K$ uncorrected	^{4}He/^{21}Ne corrected	T$_K$ corrected	T$_{Cl-Ar}$	T$_{Cl-Ar}$/T$_K$
Grant	B–230	1.816[1]	319	688	428	544	447[2]	0.82
Grant	F–110	1.816[1]	319	688	363	629	447[2]	0.71
Grant	F–165	1.816[1]	317	691	442	526	447[2]	0.85
Grant	B + 5	1.816[1]	322	684	360	633	447[2]	0.71
Grant	F–165	1.816[1]	334	668	474	486	447[2]	0.92
Grant average						**564 ± 78**		**0.80**
Carbo	M+35	1.940[1]	401	839	453	770	720[3]	0.94
Carbo	J + 41	1.940[1]	398	844	513	692	720[3]	1.04
Carbo	M + 35	1.940[1]	305	971	530	670	720[3]	1.07
Carbo	J + 41	1.940[1]	341	921	453	770	720[3]	0.94
Carbo average						**725 ± 100**		**1.00**

[1]Voshage & Feldmann (1979).
[2]Lavielle et al. (1999).
[3]Vilcsek & Wänke (1963).

1963), and 970 Ma (Goel and Kohman 1963). A summary of all ages is given in Table 3.

The uncertainties of the corrected T$_K$ only depend on the uncertainties of the N and M values (Equation 9). For the M value we use the uncertainties given by Voshage and Feldmann (1979). The uncertainties for the N values are about 14% and are dominated by the uncertainties introduced by the ^{21}Ne correction procedure (~10%). This 10% uncertainty results from the difference between the corrected ^{21}Ne values by changing the (^{22}Ne/^{21}Ne)$_{Fe + Ni}$ endmember from 1.02 to 1.05, i.e., within the reasonable limits discussed above. The total uncertainties for exposure ages are ~14% and are therefore almost entirely given by the uncertainty of the N value. When we calculate exposure ages and varying the (^{22}Ne/^{21}Ne)$_{Fe + Ni}$ endmembers ratios between 1.02 and 1.05, the final results only vary within the given 14% uncertainty, which gives confidence in the quality of the uncertainty calculations.

CONCLUSION

Based on our new precise and consistent noble gas data we determined the preatmospheric center locations, radii, and geometries of the 2 iron meteorites Grant and Carbo. Doing so, 30 aliquots of Grant and 31 aliquots of Carbo were measured for their He, Ne, and Ar isotopic concentrations. Combining the noble gas concentrations with radionuclide data demonstrates that Grant most probably experienced a single stage exposure history. For Carbo no such studies could be performed due to the lack of radionuclide data.

We demonstrated that the production of cosmogenic Ne

in iron meteorites is significantly influenced by small S- and/or P-rich inclusions like troilite and schreibersite. Even small inclusion which cannot be avoided while careful sampling can contribute up to 55% to the total ^{21}Ne concentration. For Grant and Carbo we determined an average ^{21}Ne contribution from S and P of about 20%, which corresponds to an average S and P concentration of about 0.5 wt%. Based on ^{22}Ne/^{21}Ne ratios, which are assumed to be 1.030 for Fe + Ni and 1.214 for S + P, we corrected the ^{21}Ne data for contributions from S- and/or P-rich inclusions. After correction, outliers are efficiently removed in the ^{21}Ne depth profiles for Grant and, in addition, the scatter in the Carbo depth profiles was reduced significantly. Consequently, for a first time consistent depth profiles for the production of ^{21}Ne only from Fe and Ni are given for iron meteorites.

Based on corrected ^{4}He/^{21}Ne ratios new ^{41}K-^{40}K cosmic-ray exposure ages have been calculated for Grant and Carbo. Even if the new ^{41}K-^{40}K ages are still higher than those calculated using other age systems, i.e., ^{36}Cl-^{36}Ar, ^{10}Be-^{21}Ne, and ^{26}Al-^{21}Ne, the differences are now much smaller. Consequently, the systematic discrepancies between the ^{41}K-^{40}K ages and the ^{36}Cl-^{36}Ar ages, usually attributed as long-term GCR variations (e.g., Voshage 1978, 1984; Lavielle et al. 1999) are significantly reduced when considering contributions for S and/or P-rich inclusions. However, further work to rigorously prove or reject GCR variations is currently performed.

Acknowledgments—We thank R. Wieler (ETH Zürich) for the Carbo and Grant samples. H.-E. Jennis's support for the noble gas measurements and H. Lüthis's support for sample preparation is appreciated. We also thank M. Herwegh and N. Vogel for their help on the SEM. Constructive reviews by R.C. Reedy, U. Ott, and G. Herzog are appreciated. The work is supported by the Swiss National Science Foundation.

Editorial Handling—Dr. Marc Caffee

REFERENCES

Alexander E. C., Bennett J. H., and Manuel O. K. 1968. On noble gas anomalies in the Great Namaqualand troilite. *Zeitschrift für Naturforschung* 23a:1266–1271.

Ammon K., Leya I., Lavielle B., Gilabert E., David J.-C., Herpers U., and Michel R. 2008. Cross sections for the production of helium, neon, and argon isotopes by proton-induced reactions on iron and nickel. *Nuclear Instruments and Methods in Physics Research B* 266:2–12.

Arnold J. R., Honda M., and Lal D. 1961. Record of cosmic-ray intensity in the meteorites. *Journal of Geophysical Research* 66: 3519–3531.

Begemann F. 1965. Edelgasmessungen an Eisenmeteoriten und deren Einschlüssen. *Zeitschrift für Naturforschung* 20a:950–960.

Buchwald V. F. 1975. *Handbook of iron meteorites*. University of California Press.

Buchwald V. F. 1977. The mineralogy of iron meteorites. *Philosophical Transactions of the Royal Society of London Series A* 286:453–491.

Ebert K. H. and Wänke H. 1957. Über die Einwirkung der Höhenstrahlung auf Eisenmeteorite. *Zeitschrift für Naturforschung* 12a:766–773.

Eugster O. 2003. Cosmic-ray exposure ages of meteorites and lunar rocks and their significance. *Chemie der Erde—Geochemistry* 63:3–30.

Fireman E. L. and De Felice J. 1968. Rare gases in phases of the Deelfonteine meteorite. *Journal of Geophysical Research* 73: 6111–6116.

Goel P. S. and Kohman T. P. 1963. Cosmic-ray-exposure history of meteorites from cosmogenic ^{36}Cl. In *Radioactive dating*. Vienna: International Atomic Energy Agency. pp. 413–432.

Graf T., Vogt S., Bonani G., Herpers U., Signer P., Suter M., Wieler R., and Wölfli W. 1987. Depth dependence of ^{10}Be and ^{26}Al production rates in the iron meteorite Grant. *Nuclear Instruments and Methods in Physics Research B* 29:262–265.

Hoffman J. H. and Nier A. O. 1958. Production of helium in iron meteorites by the action of cosmic rays. *Physical Review* 112: 2112–2117.

Hoffman J. H. and Nier A. O. 1959. The cosmogenic He^3 and He^4 distribution in the meteorite Carbo. *Geochimica et Cosmochimica Acta* 17:32–36.

Kwon J., Min K., Bickel P. J., and Renne P. R. 2002. Statistical methods for jointly estimating the decay constant of ^{40}K and the age of a dating standard. *Mathematical Geology* 34: 457–474.

Lavielle B., Marti K., Jeannot J.-P., Nishiizumi K., and Caffee M. 1999. The ^{36}Cl-^{36}Ar-^{40}K-^{41}K records and cosmic ray production rates in iron meteorites. *Earth and Planetary Science Letters* 170: 93–104.

Levsky L. K. and Komarov A. N. 1974. He, Ne, and Ar isotopes in inclusions of some iron meteorites. *Geochimica et Cosmochimica Acta* 39:275–284.

Leya I. 1997. Modellrechnungen zur Beschreibung der Wechselwirkungen galaktischer kosmischer Teilchenstrahlung mit Stein- und Eisenmeteoroiden. Ph.D. thesis. Universität Hannover, Germany.

Leya I., Begemann F., Weber H. W., Wieler R., and Michel R. 2004. Simulation of the interaction of galactic cosmic ray protons with meteoroids: On the production of ^{3}H and light noble gas isotopes in isotropically irradiated thick gabbro and iron targets. *Meteoritics & Planetary Science* 39:367–386.

Leya I., Lange H.-J., Neumann S., Wieler R., and Michel R. 2000. The production of cosmogenic nuclides in stony meteoroids by galactic cosmic-ray particles. *Meteoritics & Planetary Science* 35:259–286.

Leya I., Neumann S., Wieler R., and Michel R. 2001. The production of cosmogenic nuclides by galactic cosmic-ray particles for 2π exposure geometries. *Meteoritics & Planetary Science* 36:1547–1561.

Martin G. R. 1953. Recent studies on iron meteorites. IV: The origin of meteoritic helium and the age of meteorites. *Geochimica et Cosmochimica Acta* 3:288–309.

Maruoka T. and Matsuda J. 2001. New crucible for noble gas extraction. *Chemical Geology* 175:751–756.

Michel R., Peiffer F., Theis S., Begemann F., Weber H., Signer P., Wieler R., Cloth P., Dragovitsch P., Filges D., and Englert P. 1989. Production of stable and radioactive nuclides in thick stony targets (R = 15 and 25 cm) isotropically irradiated with 600 MeV protons and simulation of the production of cosmogenic nuclides in meteorites. *Nuclear Instruments and Methods in Physics Research B* 42:76–100.

Mittlefehldt D. W., McCoy T. J., Goodrich C. A., and Kracher A. 1998. Non-chondritic meteorites from asteroidal bodies. In *Planetary materials*, edited by Papike J. J. Reviews in Mineralogy and Geochemistry, vol. 36. Washington, D.C.: Mineralogical Society of America. pp. 4-1–4-195.

Sammet F. and Herr W. 1963. Studies on the cosmic-ray produced nuclides ^{10}Be, ^{26}Al and ^{36}Cl in iron meteorites. In *Radioactive*

dating. Vienna: International Atomic Energy Agency. pp. 343–354.

Schlotz R. 1977. Messungen spallogener Nuklide im Mundrabilla Eisenmeteoriten. SM thesis. Universität Heidelberg, Germany.

Schultz L. and Hintenberger H. 1967. Edelgasmessungen an Eisenmeteoriten. *Zeitschrift für Naturforschung* 22a:773–779.

Schwarzmüller J. 1970. Ein Edelgasanalysesystem mit automatischer Datenerfassung und Edelgasmessungen an Strukturelementen des Apollo 11 Mondstaubes. Universität Bern, Bern.

Signer P. and Nier A. O. 1960. The distribution of cosmic-ray-produced rare gases in iron meteorites. *Journal of Geophysical Research* 65:2947–2964.

Signer P. and Nier A. O. 1962. The measurement and interpretation of rare gas concentrations in iron meteorites. In *Researches on meteorites*, edited by Moore C. B. New York: John Wiley & Sons. pp. 7–35.

Vilcsek E. and Wänke H. 1963. ^{36}Ar, ^{36}Cl, and ^{39}Ar of meteorites. In *Radioactive dating.* Vienna: International Atomic Energy Agency. pp. 381–393.

Voshage H. 1962. Eisenmeteorite als Raumsonden für die Untersuchung des Intensitätsverlaufes der kosmischen Strahlung während der letzten Milliarden Jahre. *Zeitschrift für Naturforschung* 17a:422–432.

Voshage H. 1967. Bestrahlungsalter und Herkunft der Eisenmeteorite. *Zeitschrift für Naturforschung* 22a:477–506.

Voshage H. 1978. Investigations on cosmic-ray-produced nuclides in iron meteorites, 2. New results on ^{41}K/^{40}K-^{4}He/^{21}Ne exposure ages and the interpretation of age distributions. *Earth and Planetary Science Letters* 40:83–90.

Voshage H. 1984. Investigation of cosmic-ray-produced nuclides in iron meteorites, 6. The Signer-Nier model and the history of the cosmic radiation. *Earth and Planetary Science Letters* 71:181–194.

Voshage H. and Feldmann H. 1978. Investigations on cosmic-ray-produced nuclides in iron meteorites, 1. The measurement and interpretation of rare gas concentrations. *Earth and Planetary Science Letters* 39:25–36.

Voshage H. and Feldmann H. 1979. Investigations on cosmic-ray-produced nuclides in iron meteorites, 3. Exposure ages, meteoroid sizes and sample depth determined by mass spectrometric analyses of potassium and rare gases. *Earth and Planetary Science Letters* 45:293–308.

Voshage H. and Hintenberger H. 1961. Massenspektrometrische Isotopenhäufigkeitsmessungen an Kalium aus Eisenmeteoriten und das Problem der Bestimmung der ^{41}K-^{40}K Strahlungsalter. *Zeitschrift für Naturforschung* 16a:1042–1053.

Wieler R. 2002. Cosmic-ray-produced noble gases in meteorites. In *Noble gases*, edited by Porcelli D. P., Ballentine C. J., and Wieler R. Reviews in Mineralogy and Geochemistry, vol. 47. pp. 125–170.

Xue S., Herzog G. F., Souzis A., Ervin M. H., Lareau R. T., Middleton R., and Klein J. 1995. Stable magnesium isotopes, ^{26}Al, ^{10}Be, and ^{26}Mg/ ^{26}Al exposure ages of iron meteorites. *Earth and Planetary Science Letters* 136:397–406.